

Rapid Online Identification of Non-Linear Current-Controller Bandwidth in STATCOM Application

Hikmat Basnet 
Department of
Electrical Engineering
Tampere University
Tampere, Finland
hikmat.basnet@tuni.fi

Matias Berg
GE Vernova
Tampere, Finland
matias.berg@ge.com

Minh Tran 
Department of
Electrical Engineering
Tampere University
Tampere, Finland
minh.tran@tuni.fi

Tomi Roinila 
Department of
Electrical Engineering
Tampere University
Tampere, Finland
tomi.roinila@tuni.fi

Abstract—Control bandwidth plays an important role in the operation of a static synchronous compensator (STATCOM). The bandwidth not only defines how fast the controller reacts to the changes in the power requirements, but it is also an important factor determining the linear operating region of the controller. As the system parameters often varies over time, online measurement of the bandwidth is most desired. Recent studies have presented broadband methods such as the pseudo-random binary sequence (PRBS) and Fourier techniques which can be applied to measure the controller bandwidth. In the method, a PRBS perturbation is added to the controller reference current, the resulting output current is measured, and Fourier methods are applied to compute the control-to-output frequency response. The PRBS usually produces the frequency response rapidly and accurately, but the method often requires a relatively high perturbation amplitude which can easily violate the normal system operation. This paper proposes the use of a discrete-interval binary sequence (DIBS) for this application to minimize the injection. The DIBS is a binary sequence that has been computer-optimized to maximize the energy at specified harmonic frequencies without increasing the signal amplitude in the time-domain. Experimental results based on a three-phase STATCOM at different grid inductances are presented to demonstrate the effectiveness of the proposed method.

Index Terms—STATCOM, Deadbeat Control, Online Identification, Control Bandwidth, PRBS

I. INTRODUCTION

A STATCOM is a widely adopted power-electronics-based device in grid applications used to provide reactive power support, maintain the bus voltage, and improve the power quality. The device is comprised of a voltage source converter (VSC) with a DC-link capacitor on its DC side. Controlling the current, the STATCOM can either absorb or inject reactive power into the grid [1].

Generally, a current controller can be classified either as a linear controller or a non-linear controller [2]. A Linear controller such as the proportional-integral (PI) controller can be typically analyzed using analytical transfer function model if the parameter values are known [3]. A non-linear controller such as the deadbeat controller, on the other hand, can be extremely complex to be analyzed analytically even if the

parameter values are known [4]. As a result, it is difficult to determine, for example, the linear operating region of such a non-linear controller. In both cases the system parameter values usually vary over time, and therefore, real-time non-parametric methods to dynamically characterize the controller operation are most desired.

One of the important parameter defining the controller dynamics and the operation of the STATCOM is the control bandwidth. The control bandwidth provides vital information such as the operating range as well as the speed of the controller. The control bandwidth is often significantly affected by the change in the grid impedance and may result in poor dynamic performance during the variations in the grid impedance [5]. Power-electronics-based renewable energy integrated to the grid increases the effective grid inductance, thus increasing the X/R ratio [6]. Increase in the X/R ratio not only declines the reactive power requirement of the STATCOM but also impacts the controller's performance [7], [8]. Hence, it is imperative to determine the effective control bandwidth in order to operate the controller efficiently.

The controller bandwidth can be evaluated by measuring the control-to-output frequency response [9]. One method to measure the controller bandwidth is to add a sinusoidal voltage into the controller reference, measuring the output, and applying Fourier methods [10], [11]. However, applying a sinusoidal injection is not practical because the signal has energy only at one frequency, and thus, measuring a wide frequency band becomes very time consuming [12]. Another problem using the sinusoid is that implementing such an injection in practice is very complex especially when using the existing converter in the system.

Recent studies have presented various power-electronics applications in which the frequency response of interest has been measured by using broadband perturbations such as the pseudo-random binary sequence (PRBS) [13]–[15]. In the method, the sine sweep has been replaced by the broadband perturbation, and Fourier techniques have been applied to obtain the frequency response. As the PRBS contains energy at

several frequencies, the frequency response can be measured in a fraction of time compared to the sinusoidal injections. The drawback using the PRBS is, however, that the sequence energy is spread over multiple harmonic frequencies. In order to increase the signal energy, and therefore, the signal-to-noise ratio, either the PRBS amplitude has to be increased or more perturbation periods and averaging has to be applied [16]. Increasing the amplitude may force the system out of its nominal operating range and increasing the periods requires high computing and processing power which complicates the practical implementation [17].

This paper proposes the use of a discrete-interval binary sequence (DIBS) to measure the current controller bandwidth in a STATCOM application. The DIBS is a computer-optimized binary sequence in which the signal energy is maximized at user-specified harmonic frequencies without increasing the signal time-domain amplitude [17]. The DIBS has a lower frequency resolution but otherwise the perturbation has the same properties as the traditional PRBS.

The remainder of the paper is organized as follows. Section II explains the STATCOM control structure and the theory of system identification technique. Section III introduces the applied methodology for the online identification of the closed loop control bandwidth and also presents the formulation of the proposed DIBS excitation. Section IV presents experimental evidence based on STATCOM at different grid inductance values. Finally, section V concludes the paper.

II. THEORY

A. Control of STATCOM

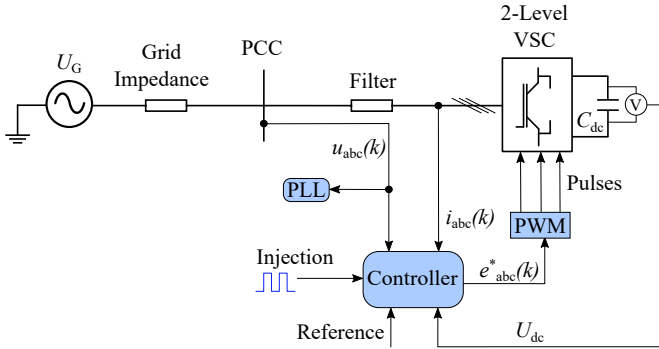


Fig. 1: STATCOM control structure

Fig. 1 shows the overall structure of the STATCOM control. The control system begins by sensing the VSC current, the DC-link voltage and the grid voltage at the point of common coupling (PCC). With the help of the phase locked loop (PLL), the grid frequency is tracked and the reference phase angle is extracted from the grid voltage. The obtained phase angle is not only used for the operation of the VSC, but also for the Park-Clarke transformations of voltage and current. By applying the Park-Clarke transformation, the reference current signal is transformed from the dq -frame to the abc -frame.

In this setup, a reference current is fed to the controller. The current controller generates the reference voltage for the PWM

modulator which provides the switching signals for the VSC. However, in practice, the performance of the control system can be negatively affected by the VSC non-linearities and the parameter mismatches [4]. The major causes of non-linearities in the grid-connected converter system are the non-ideal power switches, transformer saturation as well as the inverter dead-time [18], [19]. The combination of the non-linear deadbeat current controller and the grid inductance further increases the system non-linearity.

The controller bandwidth is an important parameter for the controller operation as the bandwidth defines how fast the controller can react to the system parameter changes. In addition, it is important to accurately know the bandwidth as it provides the linear operating region of the controller. Accurate information of the controller bandwidth enables optimal design of the outer control loop such as the reactive power controller or the AC voltage controller in the case of STATCOM. As the system parameters most often vary over time, online methods to obtain the controller bandwidth would be most desired.

B. Controller Bandwidth Measurement

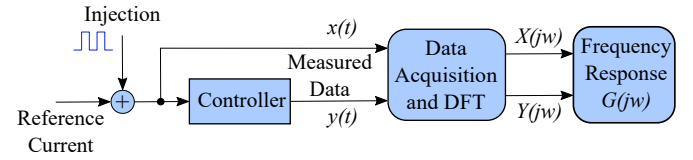


Fig. 2: Frequency response measurement setup

The controller bandwidth in a STATCOM application can be estimated by obtaining the control-to-output frequency response. Fig. 2 shows a conceptual diagram for obtaining the frequency response by applying an external perturbation. In the method, an excitation current is placed on top of the controller reference current. The output current response $y(t)$ is measured together with the applied injection $x(t)$. Then, the acquired signals are Fourier transformed and the control-to-output frequency response $G(jw)$ is obtained as

$$G(jw) = \frac{Y(jw)}{X(jw)} \quad (1)$$

where $X(jw)$ and $Y(jw)$ denote the Fourier transform of $x(t)$ and $y(t)$ respectively.

III. METHODS

A. Pseudo-Random Binary Sequence (PRBS)

Selection of the perturbation signal plays a crucial role in the identification process shown in Fig. 2. Recent studies have widely applied the PRBS to measure the frequency response of the grid-connected power electronic converters [20]–[22]. The PRBS is a periodic broadband signal that can be generated using a feedback shift-register circuit. The PRBS has energy at several frequencies, and therefore, the frequency response can be obtained in a fraction of time compared to the conventional sine-sweep technique. However, the distribution of the PRBS

energy over a wide range of harmonic frequencies results in poor SNR.

For a practical frequency-response measurement in a noisy environment, either the injection amplitude must be raised to increase the perturbation energy or the number of injection periods must be increased and averaged to reduce the effect of noise [16]. Increasing the amplitude can easily interfere with normal system operation since higher amplitude introduces non-linearities into the system. Whereas, increasing the number of injection period lengthens the measurement time, making both strategies challenging in practice [12].

B. Discrete-Interval Binary Sequence (DIBS)

The DIBS is a binary sequence where the signal is optimized to maximize the energy at user-specified harmonic frequencies. The DIBS is generated by an iterative algorithm with a selection of specific harmonic frequencies. The synthesis of the DIBS can be done in the following steps [17], [23]:

- 1) Create an N -length binary sequence d_n which has a discrete Fourier transform (DFT) of D_k .
- 2) The target is to create a sequence b_n whose Fourier coefficients are identical to that of D_k . Thus, it can be formulated as the optimization problem defined as:

$$J = \sum_{k=0}^{N-1} (|D_k| - |B_k|)^2 \quad (2)$$

where, B_k is the DFT of the optimized binary sequence b_n given by:

$$B_k = \sum_{n=1}^N b_n e^{2\pi j \frac{n-1}{N} k} \quad (3)$$

- 3) Extract the phase angles (ϕ_k) of B_k defined by:

$$B_k = |B_k| e^{j\phi_k} \quad (4)$$

- 4) Adjust ϕ_k in a series of iterations to further optimize the sequence as follows:

- a) Create a complex-value sequence given by:

$$C_k = |D_k| e^{j\phi_k} \quad (5)$$

- b) Obtain the inverse DFT of C_k as:

$$c_n = \frac{1}{N} \sum_{k=0}^{N-1} C_k e^{2\pi j \frac{n-1}{N} k} \quad (6)$$

- c) Obtain the new binary sequence, b_n by collecting the sign of c_n as:

$$b_n = \begin{cases} 1 & \text{if } c_n > 0 \\ -1 & \text{if } c_n < 0 \\ 1 \text{ or } -1 & \text{if } c_n = 0 \end{cases} \quad (7)$$

- d) Re-compute B_k and ϕ_k from the obtained sequence b_n until ϕ_k does not change.

Fig. 3 shows samples of the PRBS and DIBS both in the time and frequency domain. Both sequences are generated at

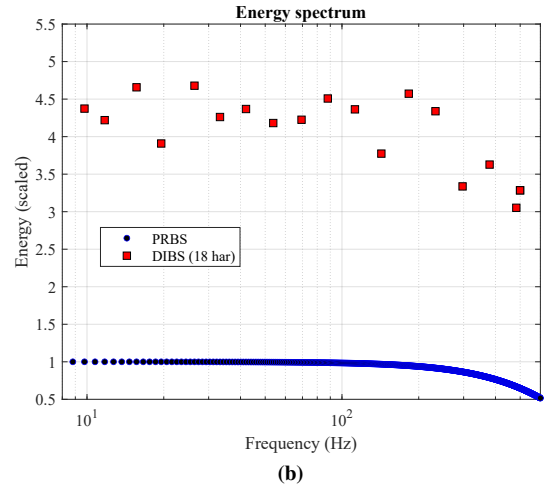
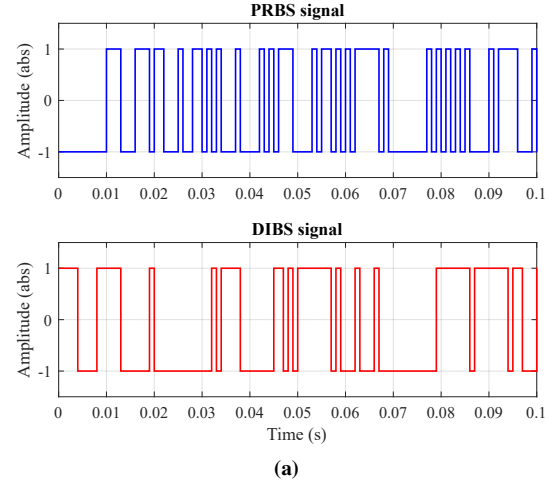


Fig. 3: Samples of PRBS and DIBS in the time domain and the frequency domain

1 kHz and they both have the same sequence length of 1023 bits. For the DIBS, 18 harmonics were logarithmically selected over 1 kHz bandwidth and the signal energy was maximized at those frequencies. As the figure shows, both signals have the same time-domain amplitude but the DIBS has approximately 4-5 times more spectral energy at the specified frequencies.

IV. EXPERIMENTAL RESULTS

A. System Setup

Fig. 4 shows the power hardware in the loop (PHIL) experimental setup applied to demonstrate the proposed control-bandwidth measurement method in a STATCOM application. Both linear (PI) and non-linear (Deadbeat) current controllers were implemented using the Imperix BoomBox rapid control prototyping. In this experiment, the decoupled PI current controller was adopted from [24]. Whereas, the non-linear deadbeat current controller is based on [25].

The grid emulator was separately controlled using dSPACE to provide 120 V RMS phase voltage. The three phase Imperix inverter was operated as a STATCOM and its control was implemented by keeping the d -axis current reference at zero using an outer voltage control loop to maintain a constant

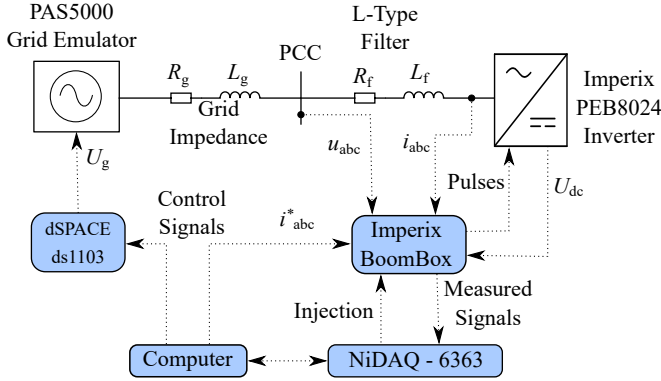


Fig. 4: Experimental setup of the STATCOM

400 V DC-link voltage. A q -axis reference current (4 A) was applied to emulate the STATCOM and provide the reactive power support. A measurement unit (NiDAQ USB-6363) was used to inject the excitation signal as well as to collect the data to and from the computer. The sampling frequency for NiDAQ card was set at 50 kHz (same as the sampling frequency of the discrete controller). The system parameter values are presented in Table I.

Table I: System Parameters

Grid	
Grid frequency, f	60 Hz
Grid voltage (rms), U_g	120 V
Grid inductance, L_g	0.38 mH
Grid resistance, R_g	0.4 Ω
STATCOM	
Switching frequency, f_{sw}	20 kHz
Sampling frequency, f_s	50 kHz
Filter inductance, L_f	2.5 mH
Filter resistance, R_f	22 m Ω
DC-link capacitor, C_{dc}	780 μ F
DC-link voltage, U_{dc}	400 V

B. Experiments

The control-to-output frequency response of the STATCOM was measured by using both the PRBS and the DIBS. Both sequences were generated at 20 kHz and they had the same sequence length of 8191 bits. For the DIBS, 18 frequency harmonics were logarithmically selected and the energy at those frequencies was maximized. Both excitations were applied with similar amplitude. The amplitude (0.1 A) was selected so that the phase current did not deviate from its nominal value more than 2.5 %. The excitation variables are presented in Table II.

Both the PRBS and the DIBS were separately injected into the q -axis reference current. Both the perturbed input reference current as well as the output q -axis current were measured

Table II: Excitation Variables

Parameter	PRBS	DIBS
Injection amplitude	0.1 A	0.1 A
Generation frequency, f_{gen}	20 kHz	20 kHz
Sequence Length, N	8191 bits	8191 bits
No. of harmonics	8191	18
Injection periods	3	3

using the NiDAQ measurement card. The measured input and the output signals were Fourier transformed and averaged over the applied injection periods.

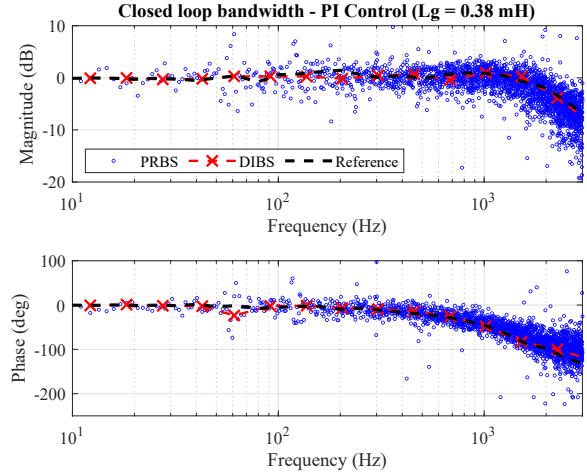


Fig. 5: Control-to-output frequency response with PI controller at $L_g = 0.38$ mH ($X_g/R_g = 0.36$)

Fig. 5 shows the q -axis control-to-output frequency response of the STATCOM with a PI current controller. The reference response shown by the black dashed line was obtained using a commercial frequency response analyzer (Venable-3120) which is based on the sine-sweep perturbation of 0.1 A amplitude. As the figure demonstrates, the PRBS shows a large error in the measured frequency-response. This is because the PRBS does not have enough energy due to presence of external noise. On the other hand, the applied DIBS has approximately 4-5 times more energy at the specified frequencies, and therefore, produces higher SNR. As a result, the curve obtained by the DIBS, follows the reference more consistently providing the bandwidth much more accurately.

C. Test Cases

Four different test cases shown in Table III were applied to further demonstrate the efficiency of the proposed bandwidth-measurement method implementing a non-linear deadbeat current controller. The nominal grid inductance (L_g) and grid resistance (R_g) in test case-1 are the parameters of the 1:1 coupling transformer connected at the PCC. Different test cases were implemented by adding an inductor of different sizes in series with the coupling transformer, that is, emulating

the network from more resistive (smaller X/R ratio) in test case-1 to more inductive (larger X/R ratio) in test case-4.

Table III: Test Cases

Test	L_g (mH)	R_g (Ω)	X_g/R_g
Case-1	0.38	0.4	0.36
Case-2	2.38	0.4	2.34
Case-3	4.68	0.4	4.41
Case-4	8.68	0.4	8.18

Fig. 6 shows the q -axis control-to-output frequency response of the STATCOM with a non-linear deadbeat current controller. In this example the PRBS shows large deviations in the gain and even larger deviations in the phase of the measured response. However, the curve obtained by the DIBS is consistent showing only a very little variance in the obtained curves.

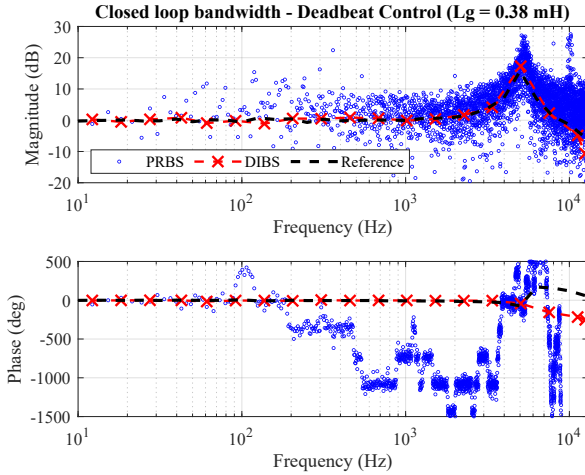


Fig. 6: Control-to-output frequency response with Deadbeat controller at $L_g = 0.38$ mH ($X_g/R_g = 0.36$)

At low frequencies where the influence of nonlinearities is more significant, the frequency response obtained by the PRBS is more distorted than that obtained by the DIBS. Although, at high frequencies the impact of nonlinearities is lower, due to the small injection period the PRBS shows larger error while the DIBS shows negligible error in the measured frequency response. This indicates that the DIBS is effective even when the non-linearities are prominent.

Fig. 7 shows the control-to-output frequency response at increased grid inductance, $L_g = 2.38$ mH (test case-2). The curves in Fig. 7 show the similar results compared to the previous examples; the DIBS provides improved measurement results whereas the PRBS fails. The frequency response measurement using the PRBS shows significant deviations especially in the phase of the measured response compared to the one using the DIBS. It can also be seen that the controller bandwidth decreased from approximately 10 kHz in test case-1 to about 7.5 kHz in test case-2.

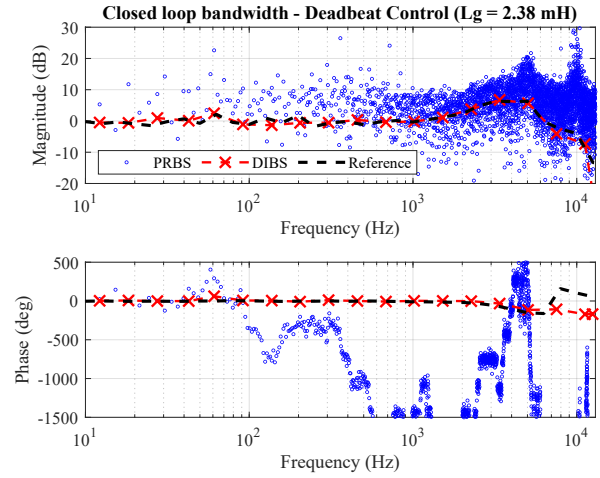


Fig. 7: Control-to-output frequency response with Deadbeat controller at $L_g = 2.38$ mH ($X_g/R_g = 2.24$)

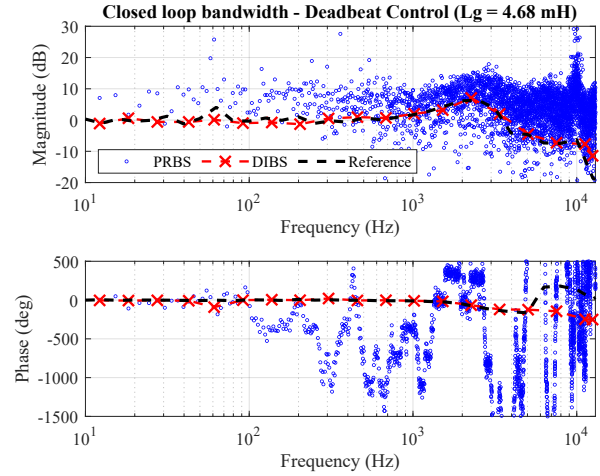


Fig. 8: Control-to-output frequency response with Deadbeat controller at $L_g = 4.68$ mH ($X_g/R_g = 4.41$)

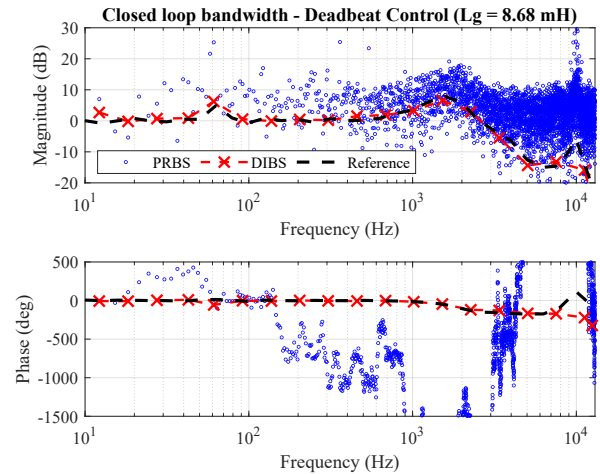


Fig. 9: Control-to-output frequency response with Deadbeat controller at $L_g = 8.68$ mH ($X_g/R_g = 8.18$)

Since the bandwidth of the control system is restricted by the grid impedance, increase in the grid inductance further declines the controller bandwidth. Fig. 8 shows the test case-3 ($L_g = 4.68$ mH), where the maximum attained bandwidth is about 3.5 kHz. Similarly, Fig. 9 shows the test case-4 ($L_g = 8.68$ mH), where the maximum bandwidth attained by the controller decreased to about 2.6 kHz. Moreover, the distortion is prominent in the frequency response obtained by the PRBS as the grid inductance increases, while the DIBS shows consistent results.

V. CONCLUSION

Control bandwidth is an important factor in the analysis and operation of a current controller applied in a STATCOM. It is of high interest to accurately measure the bandwidth in order to determine the linear operating region of the non-linear controller and to design the outer control loop effectively. Recent studies have presented the PRBS perturbation which can be applied to rapidly obtain the controller bandwidth. The method has advantages, but it requires low noise floor. Due to the tight restrictions of the injection amplitudes during the identification, the method may not work under high external noise, that is, when the noise floor is increased.

This paper has proposed an effective method based on the DIBS perturbation and Fourier techniques to accurately measure the control-to-output frequency response in a STATCOM application employing non-linear controller. The DIBS is a computer-optimized pseudo-random sequence in which the spectral energy can be increased at specific frequency harmonics without increasing the signal amplitude in the time-domain. The experimental results clearly showed the superiority of the DIBS injection compared to the conventional PRBS.

REFERENCES

- [1] E. H. Watanabe, M. Aredes, P. G. Barbosa, F. K. de Araújo Lima, R. F. da Silva Dias, and G. Santos, "Flexible AC transmission systems," *Power Electronics Handbook*, pp. 851–877, 2011.
- [2] M. Parvez, M. F. Elias, N. A. Rahim, and N. Osman, "Current control techniques for three-phase grid interconnection of renewable power generation systems: A review," *Solar Energy*, vol. 135, pp. 29–42, 2016.
- [3] M. Parvez, M. F. M. Elias, N. A. Rahim, F. Blaabjerg, D. Abbott, and S. F. Al-Sarawi, "Comparative study of discrete pi and pr controls for single-phase ups inverter," *IEEE Access*, vol. 8, pp. 45 584–45 595, 2020.
- [4] Z. Wang, J. Chai, X. Xiang, X. Sun, and H. Lu, "A novel online parameter identification algorithm designed for deadbeat current control of the permanent-magnet synchronous motor," *IEEE Transactions on Industry Applications*, vol. 58, no. 2, pp. 2029–2041, 2022.
- [5] H. Alenius, M. Berg, R. Luhtala, and T. Roinila, "Stability and performance analysis of grid-connected inverter based on online measurements of current controller loop," in *Proc. Annual Conference of the IEEE Industrial Electronics Society*, vol. 1, 2019, pp. 2013–2019.
- [6] M. Berg, A. Aapro, R. Luhtala, and T. Messo, "Small-signal analysis of photovoltaic inverter with impedance-compensated phase-locked loop in weak grid," *IEEE Transactions on Energy Conversion*, vol. 35, no. 1, pp. 347–355, 2020.
- [7] S. M. Alizadeh, C. Ozansoy, and T. Alpcan, "The impact of x/r ratio on voltage stability in a distribution network penetrated by wind farms," in *Proc. Australasian Universities Power Engineering Conference*, 2016, pp. 1–6.
- [8] J. F. Morris, K. H. Ahmed, and A. Egea-Àlvarez, "Analysis of controller bandwidth interactions for vector-controlled vsc connected to very weak ac grids," *IEEE Journal of Emerging and Selected Topics in Power Electronics*, vol. 9, no. 6, pp. 7343–7354, 2021.
- [9] A. Barkley and E. Santi, "Improved online identification of switching converters using digital network analyzer techniques," in *Proc. IEEE Power Electronics Specialists Conference*, 2008, pp. 891–896.
- [10] A. Knop and F. W. Fuchs, "High frequency grid impedance analysis by current injection," in *Proc. Annual Conference of IEEE Industrial Electronics*, 2009, pp. 536–541.
- [11] S. Buso, T. Caldognetto, and D. I. Brandao, "Dead-beat current controller for voltage-source converters with improved large-signal response," *IEEE Transactions on Industry Applications*, vol. 52, no. 2, pp. 1588–1596, 2016.
- [12] T. Roinila, T. Messo, R. Luhtala, R. Scharrenberg, E. C. De Jong, A. Fabian, and Y. Sun, "Hardware-in-the-loop methods for real-time frequency-response measurements of on-board power distribution systems," *IEEE Transactions on Industrial Electronics*, vol. 66, pp. 5769–5777, 2019.
- [13] N. Mohammed, M. Ciobotaru, and G. Town, "Performance evaluation of wideband binary identification of grid impedance using grid-connected inverters," in *Proc. European Conference on Power Electronics and Applications*, 2019, pp. 1–10.
- [14] L. Shelembe and P. Barendse, "An amplitude-modulated pseudo-random binary sequence approach to broadband impedance spectroscopy for photovoltaic module system identification," in *Proc. IEEE Energy Conversion Congress and Exposition*. IEEE, 2021, pp. 443–450.
- [15] I. P. Gerber, F. M. Mwaniki, and H. J. Vermeulen, "Parameter estimation of a grid-tied inverter using in situ pseudo-random perturbation sources," *Energies*, vol. 16, no. 3, pp. 1–24, 2023.
- [16] K. Godfrey, *Perturbation Signals for System Identification*. Hemel Hempstead, U.K: Prentice-Hall, 1993.
- [17] T. Roinila, M. Vilkkko, and J. Sun, "Online grid impedance measurement using discrete-interval binary sequence injection," *IEEE Journal of Emerging and Selected Topics in Power Electronics*, vol. 2, no. 4, pp. 985–993, 2014.
- [18] T. Roinila and T. Messo, "Online grid-impedance measurement using ternary-sequence injection," *IEEE Transactions on Industry Applications*, vol. 54, no. 5, pp. 5097–5103, 2018.
- [19] Z.-H. Liu, H.-L. Wei, X.-H. Li, K. Liu, and Q.-C. Zhong, "Global identification of electrical and mechanical parameters in pmsm drive based on dynamic self-learning pso," *IEEE Transactions on Power Electronics*, vol. 33, no. 12, pp. 10 858–10 871, 2018.
- [20] M. Céspedes and J. Sun, "Online grid impedance identification for adaptive control of grid-connected inverters," in *Proc. IEEE Energy Conversion Congress and Exposition*, 2012, pp. 914–921.
- [21] R. Luhtala, T. Roinila, and T. Messo, "Implementation of real-time impedance-based stability assessment of grid-connected systems using mimo-identification techniques," *IEEE Transactions on Industry Applications*, vol. 54, pp. 5054–5063, 2018.
- [22] T. Roinila, M. Vilkkko, and J. Sun, "Broadband methods for online grid impedance measurement," in *Proc. IEEE Energy Conversion Congress and Exposition*, 2013, pp. 3003–3010.
- [23] M. Tran, T. Roinila, and J. Markkula, "Realtime internal-impedance measurement of lithium-ion battery using discrete-interval-binary-sequence injection," in *Proc. IEEE Energy Conversion Congress and Exposition*, 2022, pp. 1–5.
- [24] H. Basnet, T. Roinila, H. Hafezi, R. Sallinen, and M. Tran, "Decoupled control to improve dc-link dynamics of energy-storage-equipped statcom," in *Proc. International Conference on Smart Energy Systems and Technologies*, 2022, pp. 1–6.
- [25] D. Martin and E. Santi, "Autotuning of digital deadbeat current controllers for grid-tie inverters using wide bandwidth impedance identification," *IEEE Transactions on Industry Applications*, vol. 50, no. 1, pp. 441–451, 2014.